ANNALS OF GEOPHYSICS, 56, 4, 2013, S0444; doi:10.4401/ag-6450

Special Issue: Vesuvius monitoring and knowledge

New insights into Mt. Vesuvius hydrothermal system and its dynamic based on a critical review of seismic tomography and geochemical features

Edoardo Del Pezzo[1,2,*], Giovanni Chiodini[1], Stefano Caliro[1], Francesca Bianco[1], Rosario Avino[1]

[1] *Istituto Nazionale di Geofisica e Vulcanologia, Sezione di Napoli, Osservatorio Vesuviano, Naples, Italy*

[2] *Instituto Andaluz de Geofisica, Universidad de Granada, Granada, Spain*

Article history

Received October 13, 2012; accepted February 13, 2013.

Subject classification:

Velocity tomography, Attenuation tomography, Hydrothermal system, Geochemical model.

ABSTRACT

The seismic velocity and attenuation tomography images, calculated inverting respectively P-wave travel times and amplitude spectra of local VT quakes at Mt. Vesuvius have been reviewed and graphically represented using a new software recently developed using Mathematica^{8TM}. *The 3-D plots of the interpolated velocity and attenuation fields obtained through this software evidence low-velocity volumes associated with high attenuation anomalies in the depth range from about 1 km to 3 km below the sea level. The heterogeneity in the distribution of the velocity and attenuation values increases in the volume centred around the crater axis and laterally extended about 4 km, where the geochemical interpretation of the data from fumarole emissions reveals the presence of a hydrothermal system with temperatures as high as 400-450 °C roughly in the same depth range (1.5 km to 4 km). The zone where the hydrothermal system is space-confined possibly hosted the residual magma erupted by Mt. Vesuvius during the recent eruptions, and is the site where most of the seismic energy release has occurred since the last 1944 eruption.*

1. Introduction

Mt. Vesuvius is one of the most dangerous volcanoes in the world, being located in a densely populated area radially extended less than 15 km from the crater. Scenarios associated with its plinian or subplinian eruptions (e.g. those occurred respectively in 79 and in 1631 A.D., see Scandone et al. [2008] and references therein) constitute the crucial elements for people evacuation in case of unrest. There is a strong debate about the reference scenario, which, on the other hand, needs a structural model of the volcano where details about location and dimensions of magma patches are well constrained.

In the present paper we give a novel joint interpretation of the shallow geological structure of Mt. Vesuvius, based on:

a) the seismic tomography images in velocity of Scarpa et al. [2002] and in attenuation of De Siena et al. [2009]. The seismic images in these two papers represent P-wave velocity and Pand S-wave attenuation in a rock volume centred at surface in the crater axis, extended laterally 10 km and vertically 6 km.

b) the geochemical conceptual model of the hydrothermal system [Chiodini et al. 2001, Caliro et al. 2011].

In the follow we describe the main already existing seismic tomography and geochemical results on which this review paper is based.

Previous seismic tomography results

Recently, seismic tomography studies (e.g. Auger et al. [2001], De Gori et al. [2001], Zollo et al. [2002], Scarpa et al. [2002], Capuano et al. [2003], where a collection of the main results and interpretations is also reported) evidenced the depth (about 8 km below the sea level) of the top layer of the main magma reservoir underneath Mt. Vesuvius. Petrological and volcanological studies (see e.g. Scaillet et al. [2008] and references therein) evidenced the possible presence of small magma patches at shallower depth, that, unfortunately, are still unfocused at the actual resolution scale of the tomography inversion.

Tomography inversion of first- P arrival times from microearthquakes [Scarpa et al. 2002] reaches a resolution of about 300-500 m, allowing for a precise relocation of the local seismicity, almost all of volcano-tectonic type, in two space clusters separated by a zone of positive Vp contrast. Scarpa et al. [2002] confirm the presence of a high Vp velocity body beneath the crater, already evidenced by other authors [e.g. De Gori et al. 2001, Capuano et al. 2003], laterally surrounded by lower

P-velocity volcanic rocks. The carbonate basement is positioned at 2-2.5 km beneath the sea-level, depth at which almost all the high energy and stressdrop seismicity (Del Pezzo et al. [2004] and references therein) is located in axis with the crater. More recently, a total-Q multiple resolution tomographic model of Mt. Vesuvius was obtained by De Siena et al. [2009]. These results indicate a structure compatible with that inferred by Scarpa et al. [2002], leading to comparable interpretations. In particular, high-Q almost corresponds with high velocity zones and *vice-versa*. It is noteworthy that the maximum magnitude earthquake ever recorded at Mt. Vesuvius in the last 40 years took place (October 9, 1999, M = 3.6) at a depth of about 3 km, in a volume characterized by both low attenuation and high velocity. De Gori et al. [2001], Zollo et al. [2002] and Scarpa et al. [2002] inferred from their tomography images the absence of any small shallow magma chamber favoring the interpretation in terms of a highly fractured aquifer, permeated by intense circulation of hot fluids.

Previous geochemical results

The conceptual geochemical model of the hydrothermal system was proposed by Chiodini et al. [2001] and further refined by Caliro et al. [2011]. Isotopic signatures of the two main components of fumarolic fluids, H_2O and CO_2 indicate for the water a derivation from a mixture of meteoric, arc-type magmatic water, and sea water [Caliro et al. 2011], while fumarolic CO_2 resulted compatible, at least partially, with a derivation from metamorphic reactions involving marine carbonates taking place in the thick carbonate sequence located at depths greater than 2.5 km underneath the volcano [Chiodini et al. 2001]. The occurrence of a decarbonation processes was confirmed by petrological considerations regarding the process of carbonate assimilation by Vesuvius magmas [Iacono-Marziano et al. 2008]. Temperatures ranging from 400 to 450 °C were inferred for the hydrothermal system hosted by the carbonate sequence at depths of 2-3 km b.s.l. [Chiodini et al. 2001].

2. Seismological images and hydrothermal structure

In this section we review the interpretation of the geological structure of Mt. Vesuvius, dealing with tomographic images provided by a new graphical technique [Del Pezzo and Bianco 2013].

We point out that attenuation tomography was obtained by De Siena et al. [2009] using the tomography velocity model calculated by Scarpa et al. [2002] as the base for seismic ray tracing. De Siena et al. [2009]

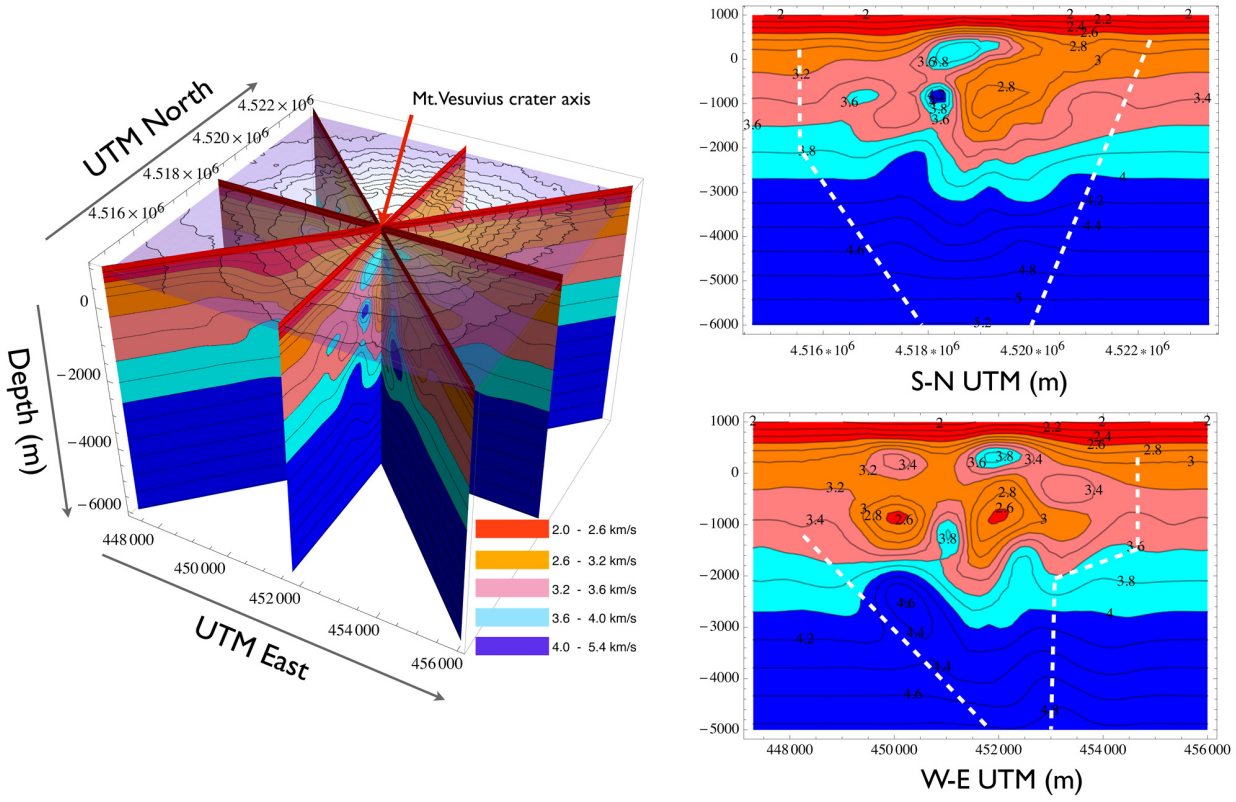

Figure 1. Left panel: 3D plot of interpolated Vp distribution in the earth volume below Mt. Vesuvius, centered at the crater axis. Easting and Northing is in UTM (meters). Depth is negative below the sea level. Mt. Vesuvius map is plotted in transparency at 800 m a.s.l. Right panels: S-N (up) and W-E sections, displaced separately for better clarity. White dashed lines confine the zone with high (300 m) resolution. On the right panels we explicitly report the isoline Vp values.

use as initial data set the same data set utilized in Scarpa et al. [2002], then select a subset of these data on the base of the signal to noise ratio of the waveforms. For this reason the images in velocity and attenuation are strictly interrelated and were jointly interpreted in De Siena et al. [2009]. Del Pezzo and Bianco [2013], in a companion paper of this special issue, describe a graphic representation of these images (both in velocity and attenuation) performed by means of the polynomial space interpolation of the tomography data utilized by Scarpa et al. [2002] and De Siena et al. [2009]. The new visualization allows for a finer visual focusing into the details of the velocity and attenuation tomographies, helping in the geological interpretations. Figures 1, 2 and 3 (similar to those included in Del Pezzo and Bianco [2013]) show respectively the 3-D P-velocity distribution, the 3-D probability of occurrence for earthquakes in the magnitude range between 2.5 and 3.6 and the 3-D S-wave Q fluctuations around the average (for any detail see Del Pezzo and Bianco [2013]).

Figure 4a shows a picture of the conceptual geochemical model of the Vesuvius hydrothermal system inferred by chemical and isotopic compositions of the fumarolic fluids discharged at bottom crater [Chiodini et al. 2001, Caliro et al. 2011]. This conceptual model provides a hot fluids magmatic source that feeds the hydrothermal aquifer where the hydrothermal liquid is composed by a mixture of meteoric water and seawater.

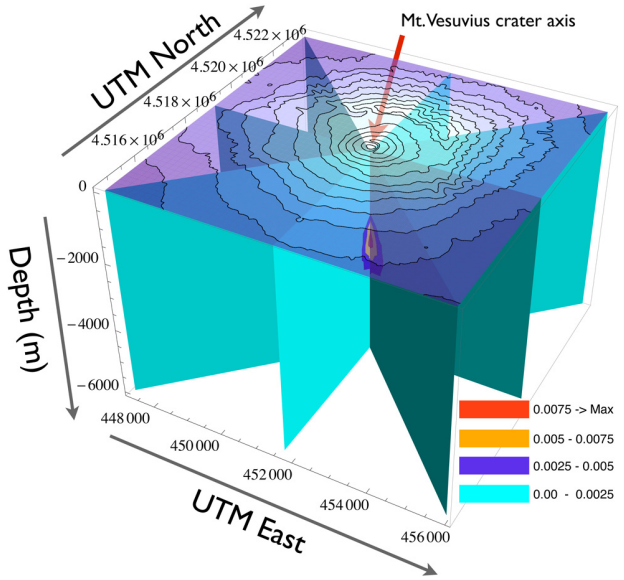

Figure 2. 3-D plot of the location probability for earthquakes with magnitude between 2.5 and 3.6 occurred between 1987 and today. Color scale represents the quantity $P\,[x, y, z, 2.5, 3.6]$ (see Del Pezzo and Bianco [2013] for all the details). Relevant energy emission corresponds to the red zone, which is strictly confined in a very narrow (500 m) and thin (1000 m) volume centered at −2500 m below the sea level.

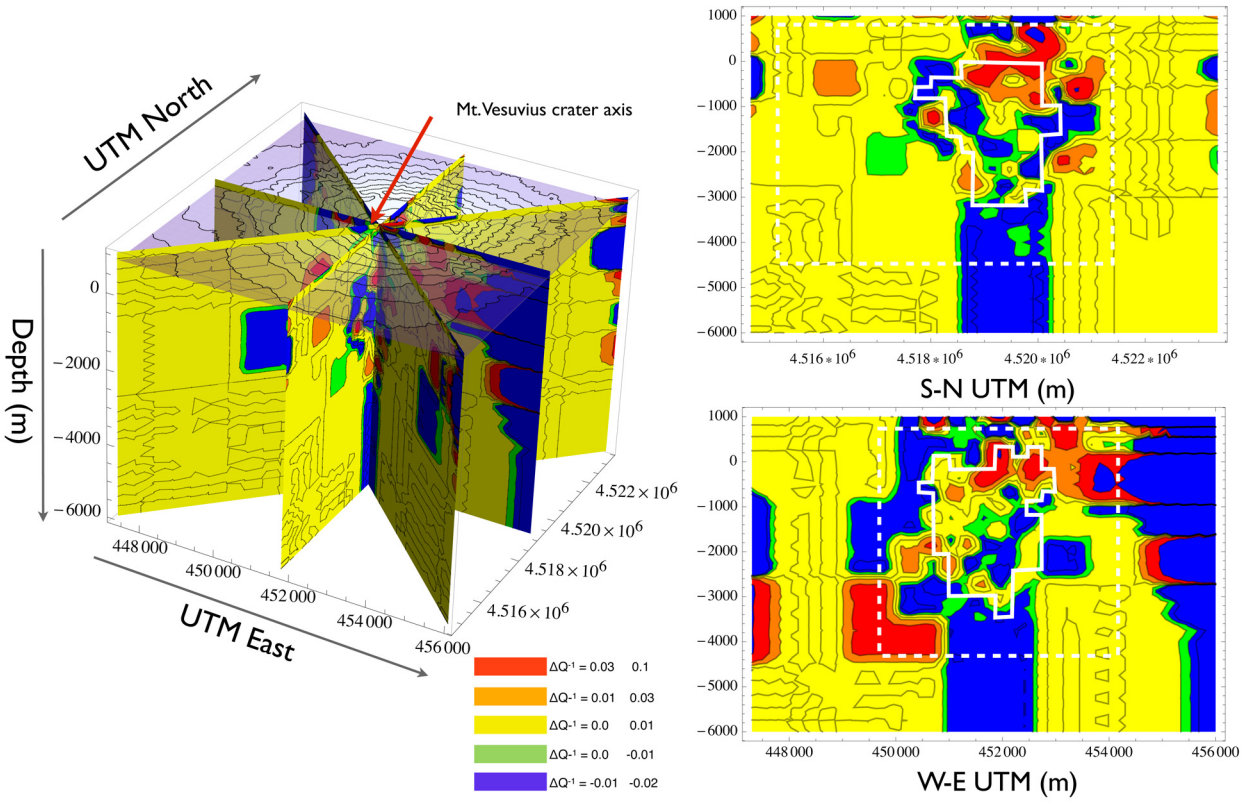

Figure 3. Left panel: 3D plot of the S-wave differential total-attenuation (total-Q - <total-Q>). Easting and Northing is in UTM (meters). Depth is negative below the sea level. Mt. Vesuvius map is plotted in transparency at 800 m a.s.l. Right panels: S-N (up) and W-E sections, displaced separately for better clarity. White dashed lines confine the zone with 1000 m resolution. Continuos line border the 500 m resolution volume.

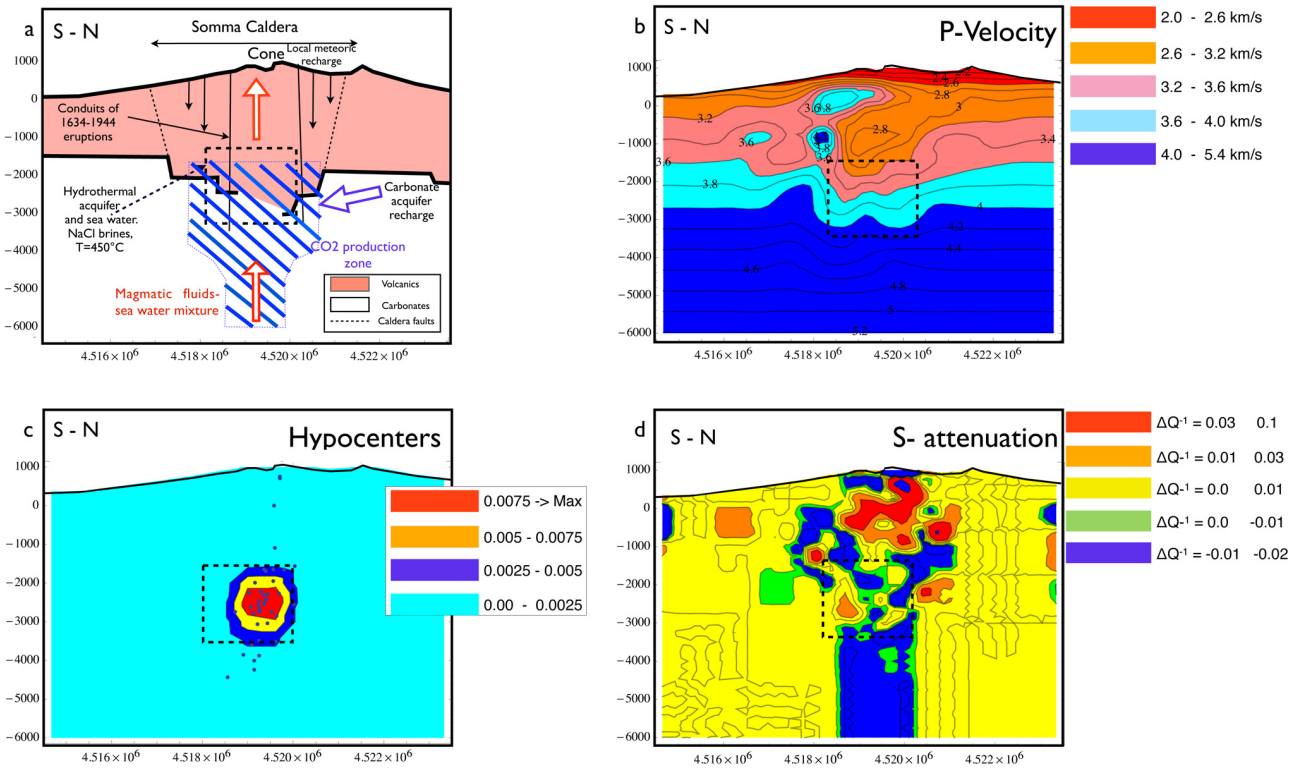

Figure 4. (a) S-N oriented conceptual geochemical model of the Vesuvius hydrothermal system inferred by chemical and isotopic compositions of fumarolic fluids discharged at bottom crater [Chiodini et al. 2001, Caliro et al. 2011]. The hydrothermal aquifer is bordered by a thick black line, which is reported for clarity also in the other three panels; (b) S-N section of the P velocity image; (c) S-N section of the location probability for earthquakes in the magnitude range between 2.5 and 3.6; (d) S-N section of the differential S wave attenuation image.

Temperature and pressure of the hydrothermal aquifer were inferred considering gas equilibria in the CO_2-CH_4-CO-H_2-H_2O gas system in the presence of *NaCl* brines. In particular, the fugacity of water, and the vapor-liquid distribution coefficients were considered to be controlled by the presence of either 3 m *NaCl* solutions or halite saturated brines. Equilibrium temperatures resulted of 445°C ± 9°C considering 3 m *NaCl* solutions and of 429°C ± 8°C for the halite-saturated brine. Such high equilibration temperatures were confirmed by the individual CO/CO_2, H_2/H_2O, and CH_4/CO_2 ratios, by the H_2-H_2S-H_2O and H_2-N_2-NH_3-H_2O gas equilibria and by the $H_2 - Ar$ geoindicator [Chiodini et al. 2001]. In addition, similar high temperatures (450-500°C) were confirmed on the basis of the *C* isotopic exchange between CH_4 and CO_2 [Fiebig et al. 2004], leaving low uncertainty on the thermal state of the Vesuvius hydrothermal system. Due to the uncertainty of the salt content of the hydrothermal liquid, the estimation of total fluid equilibrium pressure ($P_{tot} = P_{H_2O} + P_{CO_2}$) varies from 260 bar, in the case of halite saturation, to 480 bar for 3 m *NaCl* solutions [Chiodini et al. 2001]. These pressures were used to roughly estimate the depth of the hydrothermal system which resulted in the range from 1.5 to 3.5 km b.s.l. [Chiodini et al. 2001]. Considering these estimations, the hydrothermal reservoir could be roughly located within the volcanic conduit of the last eruptions, which is in turn hosted into the carbonate sequence at depths >2.5 km underneath the volcano (Figure 4a). Just above the carbonate top layer, in the zone where the volcanic conduits of the volcano are located, a clear low Vp velocity (2.8 km/s) rock volume is evidenced by the seismic tomography (Figure 4b); the relatively low velocity values in our interpretation could be due to the relatively high temperature fluids of Mt. Vesuvius hydrothermal system. It is noteworthy that also the S-wave total-Q tomography evidences a roughly co-located anomaly zone (Figure 4d). Finally, Figure 4c shows that the highest probability of occurrence for earthquakes in the magnitude range between 2.5 and 3.6 is just inside the hydrothermal system zone, at the contact between the carbonate basement and the volcanic conduits hosting the high temperature fluids.

3. Time evolution of hydrothermal system and seismicity

In addition to the strict spatial relationship between the hydrothermal fluid circulation and the occurrence of the Vesuvius seismicity, the joint analysis of the temporal evolution of the hydrothermal system and of the seismic energy release highlights another possible intriguing correlation. Immediately after the last eruption, which took place in 1944, the volcano was characterized by high temperature fumaroles (600-800°C, Figure 5a).

This observation points out that in that time volcanic vapors were hosted by the system. Successively, the unique available fumarole temperature measurement shows a sharp decrease down to the value of 290°C in 1964. Such a decrease, occurred in the early 1960s, is confirmed by the measurements sistematically performed after 1975 which from 240°C-220°C decreased down to the present time values of ≃95°C, i.e. the boiling point of the water. We can hypothesize that during the years between 1960 and 1970 the cold groundwaters present inside the carbonate formations begun to enter into the hot zones of the volcanic conduits cooling the system and in the same time increasing the fluid pressure. As a consequence of this process, an increase of the seismic energy release was generated by rock failures triggered by the fluid pressure increase. The plot of the yearly number of earthquakes registered at the station located in the Osservatorio Vesuviano old building (OVO station, data from Giudicepietro et al. [2010]) as a function of time shows indeed a corresponding marked increase in the number of the seismic events (Figure 5b). This time change in the seismicity rate has been considered with some attention due to the almost contemporaneous installation of a new kind of seismographs at OVO [Giudicepietro et al. 2010]. Even carefully considering the history of the instrument installation at OVO, we favor anyway the hypothesis that the seismicity rate change during the years between 1960 and 1970 is most probably a real process, in agreement with Giudicepietro et al. [2010]. The seismicity increase would be due to the emplacement of the hydrothermal circulation in the volcano, i.e. by the effects of the entrance into the system of the cold groundwaters of the regional aquifer, hosted by the basement, with the consequent fluid pressure increase.

More recently, the seismic activity of Mt. Vesuvius further increased up to the M=3.6 earthquake of October 9, 1999. As shown by the cumulative log of seismic energy release (Figure 6), the time interval characterized by the most intense energy release is that between the beginning of 1999 and the end of 2002. The peak of the seismic energy release of 1999 marks the beginning of evident changes in the fumarolic composition, including both an increase of the CO_2/CH_4 ratio and of the equilibrium P_{CO_2} computed within the CO_2-CH_4-CO-H_2-H_2O gas system. The CO_2/CH_4 ratio is a good tracer of magmatic fluids injection into hydrothermal systems located in active volcanoes [Chiodini 2009]. Indeed, CO_2 concentration increases due to the higher content of the magmatic component with respect to the hydrothermal one. CH_4, which originates within the hydrothermal system, can be lowered both by dilution and by the more oxidizing, transient conditions possibly caused by the arriving of SO_2 into the hydrothermal environment. This opposite behavior causes rapid increases of the fumarolic CO_2/CH_4. It is worth to note that the geochemical signals follow of some time the maximum energy release as expected because of the transferring time of the fluids from the deep seismogenetic zone of the hydrothermal system to the shallow fumarolic discharge zone. Similar anomalies accompanying volcanic unrest periods were observed also in other volcano-hydrothermal systems such as at Campi Flegrei and Panarea (Italy), Mammoth Mountain (California), Nisyros (Greece) and Mt. Baker (Washington) [Chiodini 2009, Werner et al. 2009, Chiodini et al. 2012]. It is consequently reasonably realistic that during 1999-2002 the Vesuvius hydrothermal system was affected by episodes of injection of deeper magmatic fluids. In our opinion this process both caused the increase of the P_{CO_2}, as registered by the chemical

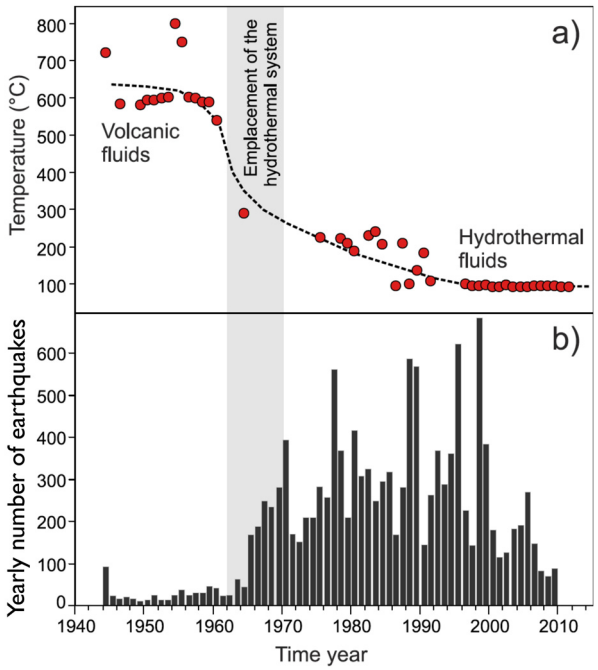

Figure 5. (a) Time behavior of the fumaroles temperature since 1944. The data before 2000 are taken from Chiodini et al. [2001], and reference therein, while the other are from Caliro et al. [2011]; (b) Number of earthquakes per year since 1944.

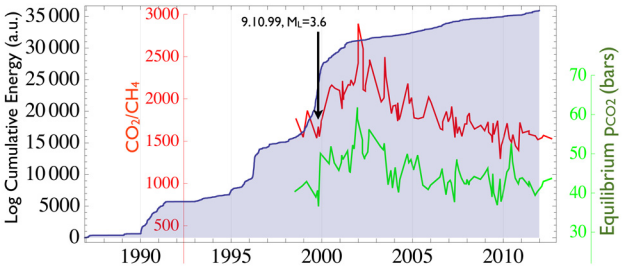

Figure 6. Cumulative seismic energy (blu line), ratio between carbon dioxide and methane (red line) and P_{CO_2} equilibrium (green line) since 1987.

variation within the CO_2-CH_4-CO-H_2-H_2O gas system, and in turn triggered the high seismicity of the period. In agreement with our interpretation, Saccorotti et al. [2002] proposed that at least a part of the seismic activity at Vesuvius is triggered by diffusion of a pressure front, possibly associated with the degassing process of the hydrothermal system.

4. Concluding remarks

This paper review previous tomographic results and geochemical features, interpreting them in a unique frame that enlightens new features which were unfocused in the previous papers on this topic. New images of the geological structure in the first 5 km below Mt. Vesuvius confirm, as described in De Siena et al. [2009], that high Q zones almost coincide with high velocity zones, eventually favoring a more grounded multi-disciplinary interpretations. Geochemical evidences, schematized in easy sketchs were thus compared with seismic tomography images, and the details of this comparison lead to the following novel conclusions:

1) a clear low Vp velocity rock volume and an S-wave total-Q anomaly, roughly located in the same zone, can be associated with the relatively high temperature fluids of the Mt. Vesuvius hydrothermal system;

2) the zones with high probability of earthquake occurrence are practically coincident with the aquifer;

3) geochemical considerations about the increase of the fumarolic CO_2/CH_4 which accompanied the largest magnitude (M=3.6) earthquake of October 9, 1999, indicate that it is quite realistic that an injection of deep magmatic fluids may have triggered the seismicity in that period.

It is also interesting to notice that the idea (already discussed by Caliro et al. [2011]) that the decrease of the temperature fumaroles (from 600 degrees in the fifties down to the water boiling point today) is strictly associated with the cold groundwater cooling of the residual magma body, is clearly confirmed in the framework of the geological structure schematized in the present paper.

Acknowledgements. This work has been partially supported by the following projects: V2-"Precursori di Eruzioni in Vulcani Quiescenti: Campi Flegrei e Vulcano". Convenzione INGV-DPC (2012-2013); EPHESTOS CGL2011-2949-C02-01 (University of Granada, Instituto Andaluz de Geofísica); MEDiterranean SUpersite Volcanoes (MED-SUV) FP7 ENV.2012.6.4-2 Grant agreement no. 308665. (European Community).

References

Auger, E., P. Gasparini, J. Virieux and A. Zollo (2001). Seismic Evidence of an Extended Magmatic Sill Under Mt. Vesuvius, Science, 294,1510-1512.

Caliro, S., G. Chiodini, R. Avino, C. Minopoli and B. Bocchino (2011). Long time-series of chemical and isotopic compositions of vesuvius fumaroles: evidence for deep and shallow processes of vesuvius fumaroles: evidence for deep and shallow processes, Annals of Geophysics, 54 (2), 137-149.

Capuano, P., P. Gasparini, A. Zollo, J. Virieux, R. Casale and M. Yeroyanni (2003). The internal structure of Mt. Vesuvius. A seismic tomography investigation, Liguori Editore, Naples.

Chiodini, G., L. Marini and M. Russo (2001). Geochemical evidence for the existence of high-temperature hydrothermal brines at Vesuvio volcano, Italy, Geochimica et Cosmochimica Acta, 65 (13), 2129-2147.

Chiodini, G. (2009). CO_2/CH_4 ratio in fumaroles a powerful tool to detect magma degassing episodes at quiescent volcanoes, Geophysical Research Letters, 36, L02302; doi:10.1029/2008GL036347.

Chiodini, G., S. Caliro, P. De Martino, R. Avino and F. Gherardi (2012). Early signals of new volcanic unrest at campi flegrei caldera? Insights from geochemical data and physical simulations, Geology, 40, 943-946.

De Gori, P., G. Cimini, C. Chiarabba, G. De Natale, C. Troise and A. Deschamps (2001). Teleseismic tomography of the campanian volcanic area and surrounding apenninic belt, Journal Of Volcanology And Geothermal Research, 109, 55-75.

Del Pezzo, E., F. Bianco and G. Saccorotti (2004). Seismic source dynamics at Vesuvius volcano, Italy, Journal of Volcanology and Geothermal Research, 133 (1-4), 23-39.

Del Pezzo, E., and F. Bianco (2013). Inside Mt. Vesuvius: a new method to look at the seismic (velocity and attenuation) tomographic imaging, Annals of Geophysics, 56 (4), S0443; doi:10.4401/ag-6449.

De Siena, L., E. Del Pezzo, F. Bianco and A. Tramelli (2009). Multiple resolution seismic attenuation imaging at Mt. Vesuvius, Physics Of The Earth And Planetary Interiors, 173, 17-32.

Fiebig, J., G. Chiodini, S. Caliro, A. Rizzo, J. Spangenberg and J.C. Hunziker (2004). Chemical and isotopic equilibrium between CO_2 and CH_4 in fumarolic gas discharges: Generation of CH_4 in arc magmatic-hydrothermal systems, Geochimica et Cosmochimica Acta, 68 (10), 2321-2334.

Giudicepietro, F., M. Orazi, G. Scarpato, R. Peluso, L. D'Auria, P. Ricciolino, D. Lo Bascio, A.M. Esposito, G. Borriello, M. Capello, A. Caputo, C. Buonocunto, W. De Cesare, G. Vilardo and M. Martini (2010). Seismological Monitoring of Mount Vesuvius (Italy): More than a Century of Observations, Seismological Research Letters, 81 (4), 625-634.

Iacono-Marziano, G., F. Gaillard, B. Scaillet, M. Pichavant and G. Chiodini (2008). Role of non-mantle CO_2 in the dynamics of volcano degassing: The Mount Vesuvius example, Geology, 37 (4), 319-322.

Saccorotti, G., G. Ventura and G. Vilardo (2002). Seismic swarms related to diffusive processes: The case of Somma-Vesuvius volcano, Italy, Geophysics, 67, 199-203.

Scaillet, B., M. Pichavant and R. Cioni (2008). Upward migration of Vesuvius magma chamber over the past 20,000 years, Nature, 455 (7210), 216-219.

Scandone, R., L. Giacomelli and F.F. Speranza (2008). Persistent activity and violent strombolian eruptions at Vesuvius between 1631 and 1944, Journal of Volcanology and Geothermal Research, 170 (3-4), 167-180.

Scarpa, R., F. Tronca, F. Bianco and E. Del Pezzo (2002). High resolution velocity structure beneath Mount Vesuvius from seismic array data, Geophysical Research Letters, 29 (21), CiteID 2040; doi:10.1029/2002GL015576.

Werner, C., W. Evans, M. Poland, D. Tucker and M.P. Doukas (2009). Long-term changes in quiescent degassing at Mount Baker Volcano, Washington, USA. Evidence for a stalled intrusion in 1975 and connection to a deep magma source, Journal of Volcanology and Geothermal Research, 186, 379-386.

Zollo, A., L. D'Auria, R. De Matteis and A. Herrero (2002). Bayesian estimation of 2-D P-velocity models from active seismic arrival time data- Imaging of the Shallow Structure of Mt.Vesuvius (Southern Italy), Geophysical Journal International, 151, 566-582.

*Corresponding author: Edoardo Del Pezzo,
Istituto Nazionale di Geofisica e Vulcanologia, Sezione di Napoli,
Osservatorio Vesuviano, Naples, Italy;
email: edoardo.delpezzo@ov.ingv.it.